

Clustering with Total Variation Graph Neural Networks

Jonas Berg Hansen and Filippo Maria Bianchi

UiT the Arctic University of Norway, Dept. of Mathematics and Statistics
{jonas.b.hansen, filippo.m.bianchi}@uit.no

Abstract

Graph Neural Networks (GNNs) are deep learning models designed to process attributed graphs. GNNs can compute cluster assignments accounting both for the vertex features and for the graph topology. Existing GNNs for clustering are trained by optimizing an unsupervised minimum cut objective, which is approximated by a Spectral Clustering (SC) relaxation. SC offers a closed-form solution that, however, is not particularly useful for a GNN trained with gradient descent. Additionally, the SC relaxation is loose and yields overly smooth cluster assignments, which do not separate well the samples. We propose a GNN model that optimizes a tighter relaxation of the minimum cut based on graph total variation (GTV). Our model has two core components: i) a message-passing layer that minimizes the ℓ_1 distance in the features of adjacent vertices, which is key to achieving sharp cluster transitions; ii) a loss function that minimizes the GTV in the cluster assignments while ensuring balanced partitions. By optimizing the proposed loss, our model can be self-trained to perform clustering. In addition, our clustering procedure can be used to implement graph pooling in deep GNN architectures for graph classification. Experiments show that our model outperforms other GNN-based approaches for clustering and graph pooling.

1 Introduction

Traditional clustering techniques partition the samples based on their features or on suitable data representations computed, for example, with deep learning models (Tian et al., 2014; Min et al., 2018; Su et al., 2022). Spectral clustering (SC) (Von Luxburg, 2007) is a popular technique that first encodes the similarity of the data features into a graph and then creates a partition based on the graph topology. Such a graph is just a convenient representation of the similarity among the samples and has no attributes on its vertices.

On the other hand, an attributed graph can represent both the relationships among samples and their features. Graph Neural Networks (GNNs) are deep learning architectures specifically designed to process and make inference on such data (Hamilton, 2020). Therefore, contrarily to traditional clustering methods, a GNN-based approach for clustering can account for both the features and the relationships among samples to generate partitions (see Fig. 1a).

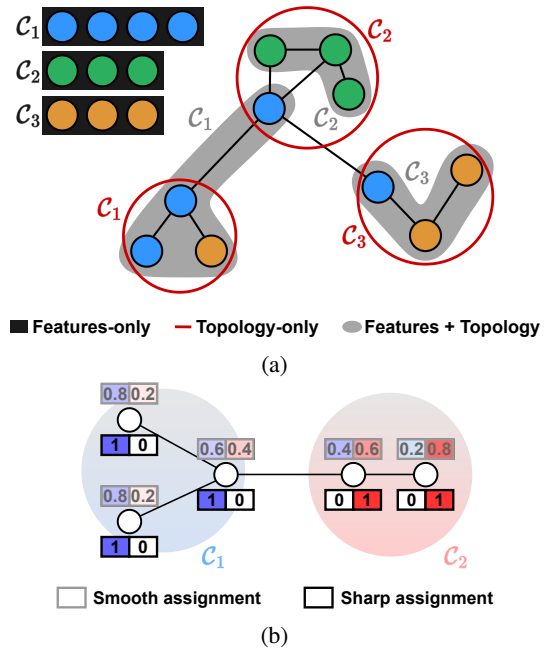


Figure 1: **a)** Most clustering methods partition the data only based on the features (■). SC partitions the vertices of the graph based on its topology (■). GNN-based clustering accounts both for the vertex features and the graph topology (■). **b)** An example of the difference between smooth and sharp cluster assignments. Especially at the edge of a cluster, the smooth assignments give large weights to more than one cluster.

Similarly to other deep learning architectures for clustering (Shaham et al., 2018; Kampffmeyer et al., 2019), GNNs are trained end-to-end and return the soft cluster assignments as part of the output. The existing GNN clustering approaches compute cluster assignments from the vertex representations generated by the message passing (MP) layers and, then, optimize the assignments with an unsupervised

loss inspired by SC (Bianchi et al., 2020; Tsitsulin et al., 2020; Bianchi, 2022; Duval and Malliaros, 2022). The SC objective benefits from the smoothing operations performed by the MP layers, which minimize the local quadratic variation of adjacent vertex features. However, this approach produces smooth cluster assignment vectors that are less informative as they do not separate well the samples (see Fig.1b). Indeed, the SC objective is known to give a loose approximation of the optimal partition defined in terms of the minimum cut (Rangapuram et al., 2014).

Contributions We propose a novel GNN-based clustering approach that generates cluster assignments by optimizing the graph total variation (GTV). Compared to SC, GTV trades a closed-form solution with a tighter continuous relaxation of the optimal minimum cut partition (Hein and Setzer, 2011). Notably, an optimization objective with a closed-form solution is not particularly useful for a GNN trained with gradient descent.

We design an unsupervised loss function for minimizing the GTV that is GNN-friendly as it avoids numerical issues during gradient descent and assumes values in a well-defined range, making it suitable to be combined with other losses. Our GNN yields sharp cluster assignments by minimizing the ℓ_1 norm of their differences. Clearly, the minimization of the GTV is hindered when the cluster assignments derive from the smooth representations computed by traditional MP layers. To address this issue, we propose a new MP layer that minimizes the ℓ_1 norm of the difference between adjacent vertex features.

By optimizing the proposed loss, we can train a GNN end-to-end to perform vertex clustering. In addition, by coarsening the graph according to the learned partition we can perform hierarchical graph pooling (Grattarola et al., 2022) in deep GNN architectures for graph-level tasks, such as graph classification. In this case, the proposed loss is combined with an additional supervised loss, such as the cross-entropy. Experiments show the superiority of the proposed approach compared to the other GNN methods for clustering and for graph pooling.

2 Background

A graph is represented by a tuple $\mathcal{G} = \{\mathcal{V}, \mathcal{E}\}$ where \mathcal{V} and \mathcal{E} are the vertex and edge sets, respectively, $|\mathcal{V}| = N$, and $|\mathcal{E}| = E$. The adjacency matrix $\mathbf{A} \in \mathbb{R}^{N \times N}$ with elements $a_{i,j} \in \{0, 1\}$ defines the graph connectivity. In an attributed graph, each vertex i is associated with a feature vector $\mathbf{x}_i \in \mathbb{R}^F$. Feature vectors are often grouped in a matrix $\mathbf{X} \in \mathbb{R}^{N \times F}$. The soft cluster assignment matrix is $\mathbf{S} \in \mathbb{R}^{N \times K}$, where K is the number of clusters and $s_{i,j} \in [0, 1]$ is the membership of vertex i to cluster j . The combinatorial Laplacian is $\mathbf{L} = \mathbf{D} - \mathbf{A}$ and $\tilde{\mathbf{A}} = \mathbf{D}^{-1/2} \mathbf{A} \mathbf{D}^{-1/2}$ is the symmetric degree normalization of \mathbf{A} .

2.1 Graph cuts

The task of finding K clusters of similar size can be cast into the balanced K -cut problem, defined as a ratio of two set functions:

$$C = \min_{C_1, \dots, C_K} \sum_{k=1}^K \frac{\text{cut}(C_k, \bar{C}_k)}{\hat{S}(C_k)}, \quad (1)$$

where $\text{cut}(C_i, C_j)$ counts the volume of edges connecting the two sets of vertices $C_i, C_j \subset \mathcal{V}$, \bar{C}_k is the complement of set k , and $\hat{S}(\cdot) : 2^{\mathcal{V}} \rightarrow \mathbb{R}_+$ is a submodular set function that balances the size of the clusters in the partition (Hein and Setzer, 2011). Depending on the choice of $\hat{S}(\cdot)$ different cuts are obtained, such as the ratio cut for $\hat{S}(C_k) = |C_k|$, and the normalized cut for $\hat{S}(C_k) = \text{vol}(C_k)$ (Von Luxburg, 2007). Of particular interest for us is the Cheeger cut, also known as Balanced cut or Ratio Cheeger cut, where $\hat{S}(C_k) = \min\{|C_k|, |\bar{C}_k|\}$ penalizes the formation of very large clusters. A variant of the Cheeger Cut, called *Asymmetric Cheeger cut*, encourages an even partition by letting $\hat{S}(C_k) = \min\{(K-1)|C_k|, |\bar{C}_k|\}$ (Bresson et al., 2013).

2.2 Tight relaxation of Asymmetric Cheeger cut

Let the numerator in (1) be expressed in matrix form as

$$\text{cut}(C_k, \bar{C}_k) = \sum_{i \in C_k, j \in \bar{C}_k} a_{ij} (1 - z_i z_j) = \mathbf{z}^T \mathbf{L} \mathbf{z}, \quad (2)$$

with $z_i, z_j \in \{-1, 1\}$ (derivation in the supplementary). The common relaxation done in spectral clustering (SC) is:

$$\min_{\mathbf{z} \in \{-1, 1\}^N} \frac{\mathbf{z}^T \mathbf{L} \mathbf{z}}{\hat{S}(C_k)} \rightarrow \min_{\mathbf{s} \in \mathbb{R}^N} \frac{\mathbf{s}^T \mathbf{L} \mathbf{s}}{S(C_k)} \quad (3)$$

where $S(C_k)$ is the continuous counterpart of $\hat{S}(C_k)$. What the SC relaxation actually does, is to apply Laplacian smoothing to a graph signal \mathbf{s} by minimizing its local quadratic variation (LQV). The LQV defined in terms of the combinatorial Laplacian reads

$$\mathbf{s}^T \mathbf{L} \mathbf{s} = \frac{1}{2} \sum_{(i,j) \in \mathcal{E}} a_{i,j} (s_i - s_j)^2. \quad (4)$$

From the graph signal processing perspective, Laplacian smoothing applies to a graph signal a low-pass filter with response $(1 - \lambda_i)$, where λ_i is the i -th eigenvalue of the Laplacian (Tremblay et al., 2018).

Despite offering a closed-form solution, SC gives a loose approximation of the solution of the discrete optimization problem (Hein and Setzer, 2011). Let $\mathbf{s}_k \in \mathbb{R}^N$ be the soft assignment vector for the k -th cluster. A tighter continuous relaxation of the Asymmetric Cheeger cut problem is given by Bresson et al. (2013):

$$\min_{\mathbf{s}_k \in \mathbb{R}^N} \sum_{k=1}^K \frac{\|\mathbf{s}_k\|_{\text{GTV}}}{\|\mathbf{s}_k - \text{quant}_{\rho}(\mathbf{s}_k)\|_{1,\rho}} \text{ s.t. } \sum_k \mathbf{s}_k = \mathbf{1}_N. \quad (5)$$

In the numerator, $\|\mathbf{s}_k\|_{\text{GTV}} = \sum_{i,j} a_{i,j} |s_{i,k} - s_{j,k}|$ measures the graph total variation (GTV) of the soft assignments to cluster k . In the denominator, $\text{quant}_\rho(\mathbf{s}_k)$ denotes the ρ -quantile of \mathbf{s}_k , i.e., the $(q+1)$ st largest value in \mathbf{s}_k with $q = \lfloor N/(\rho+1) \rfloor$, while $\|\cdot\|_{1,\rho}$ denotes an asymmetric ℓ_1 norm, which for a vector $\mathbf{x} \in \mathbb{R}^N$ is

$$\|\mathbf{x}\|_{1,\rho} = \sum_{i=1}^N |x_i|_\rho, \text{ where } |x_i|_\rho = \begin{cases} \rho x_i, & x_i \geq 0 \\ -x_i, & x_i < 0 \end{cases}. \quad (6)$$

When $\rho = K-1$, the denominator in (5) encourages balanced partitions, i.e., clusters having similar sizes, and prevents the two common *degenerate solutions*: i) all samples collapsing into the same cluster (e.g., $\mathbf{s}_i = [1, 0, \dots, 0], \forall i$), and ii) samples uniformly assigned to all clusters ($\mathbf{s}_i = [1/K, 1/K, \dots, 1/K], \forall i$).

Differently from SC, (5) minimizes the ℓ_1 rather than the ℓ_2 distance between components of \mathbf{s} that are adjacent on the graph. Minimizing GTV yields sharper cluster assignments and achieves a tighter relaxation of the balanced K -cut problem compared to SC (Rangapuram et al., 2014; Bresson et al., 2013). However, contrarily to SC, (5) is non-convex and is optimized through iterative updates.

2.3 Clustering with Graph Neural Networks

To leverage the graph topology for learning vertex representations, GNNs implement message-passing (MP) layers. Typically, an MP layer collects information from the neighbours to update the representation of each vertex (Hamilton, 2020). An example of an MP layer is the Graph Convolutional Network (GCN) by Kipf and Welling (2017):

$$\mathbf{X}^{(\text{out})} = \sigma(\tilde{\mathbf{A}}' \mathbf{X}^{(\text{in})} \Theta_{\text{MP}}) \quad (7)$$

where $\mathbf{A}' = \mathbf{A} + \mathbf{I}_N$ and $\Theta_{\text{MP}} \in \mathbb{R}^{F_{\text{in}} \times F_{\text{out}}}$ are learnable parameters. It can be shown that a GCN layer applies Laplacian smoothing on the vertex features \mathbf{X} ; see Wu et al. (2019); Nt and Maehara (2019); Li et al. (2018); Bianchi et al. (2021) for detailed discussions. For example, Ma et al. (2021) shows that the l -th GCN layer updates of the vertex features as

$$\mathbf{X}^{(l+1)} = (\mathbf{I} - \delta \tilde{\mathbf{A}}') \mathbf{X}^{(l)}, \quad (8)$$

which is actually one gradient descent step of size δ in the optimization of problem

$$\min_{\mathbf{X}} \text{Tr}(\mathbf{X}^T (\mathbf{I} - \tilde{\mathbf{A}}') \mathbf{X}). \quad (9)$$

A similar derivation is shown for GAT (Veličković et al., 2017) and APPNP (Klicpera et al., 2018), which optimize a slightly different problem. For example, each iteration in APPNP is a gradient descent step for

$$\min_{\mathbf{X}} \|\mathbf{X} - \mathbf{X}^{(0)}\|_F^2 + (1/\alpha - 1) \text{Tr}(\mathbf{X}^T (\mathbf{I} - \tilde{\mathbf{A}}') \mathbf{X}), \quad (10)$$

where $\mathbf{X}^{(0)}$ are the original vertex features and $\alpha \in [0, 1]$. Both (9) and (10) minimize the LQV defined in (4) by reducing the ℓ_2 distance between the features of adjacent vertices, i.e., they perform Laplacian smoothing.

After applying a stack of L MP layers, the assignment matrix \mathbf{S} is obtained by passing the updated vertex features to some function f , typically a multi-layer perceptron (MLP) with a `softmax` activation, that produces a K -dimensional vector for each vertex. Importantly, since the MP layers perform Laplacian smoothing and f is a smooth function, the cluster assignments generated from $\mathbf{X}^{(L)}$ comply with the SC definition. Nevertheless, minimizing the LQV of $\mathbf{X}^{(L)}$ is not the same as minimizing the LQV of \mathbf{S} directly. In addition, the size of the clusters must be balanced and degenerate solutions avoided. For these reasons, the assignments \mathbf{S} are further optimized through unsupervised loss functions. For instance, MinCutPool (Bianchi et al., 2020) optimizes the following loss

$$\underbrace{-\frac{\text{Tr}(\mathbf{S}^T \tilde{\mathbf{A}} \mathbf{S})}{\text{Tr}(\mathbf{S}^T \tilde{\mathbf{D}} \mathbf{S})}}_{\mathcal{L}_c} + \underbrace{\left\| \frac{\mathbf{S}^T \mathbf{S}}{\|\mathbf{S}^T \mathbf{S}\|_F} - \frac{\mathbf{I}_K}{\sqrt{K}} \right\|_F}_{\mathcal{L}_o}, \quad (11)$$

where $\|\cdot\|_F$ indicates the Frobenius norm and $\tilde{\mathbf{D}} = \text{diag}(\tilde{\mathbf{A}} \mathbf{1})$. The \mathcal{L}_c term encourages strongly connected components to be clustered together, while \mathcal{L}_o is a balancing term that promotes equally-sized clusters and helps to avoid degenerate solutions. Similarly, DMoN (Tsitsulin et al., 2020) optimizes a two-termed loss

$$\underbrace{-\frac{\text{Tr}(\mathbf{S}^T \mathbf{A} \mathbf{S} - \mathbf{S}^T \mathbf{d}^T \mathbf{d} \mathbf{S})}{2|\mathcal{E}|}}_{\mathcal{L}_m} + \underbrace{\frac{\sqrt{K}}{N} \left\| \sum_i \mathbf{S}_i^T \right\|_F}_{\mathcal{L}_r} - 1, \quad (12)$$

where \mathbf{d} is the degree vector of \mathbf{A} , \mathcal{L}_m pushes strongly connected components to the same cluster, and \mathcal{L}_r is a regularization term that penalizes the degenerate solutions.

The losses in (11) and (12) are closely related to SC, from which the problem of smooth cluster assignments is inherited. In addition, being trained with gradient descent, the GNNs do not exploit the closed-form solution of SC. This motivates relying on GTV to perform clustering with a GNN.

3 Total Variation Graph Neural Network

In this section, we present the two core components of the Total Variation Graph Neural Network (TVGNN). First, we introduce the unsupervised clustering loss inspired by the GTV relaxation. Then, we present a novel MP layer to be used in conjunction with the proposed loss. We conclude by showing two specific TVGNN architectures that can be used for vertex clustering and for graph classification.

3.1 The loss function

In principle, the optimization of the objective in (5) yields a balanced partition with sharp transitions in the assignment vectors of adjacent vertices belonging to different clusters. However, the relaxed Asymmetric Cheeger Cut expression is ill-suited for the stochastic gradient descent used to train a GNN, due to potential numerical issues in the proximity of the degenerate solutions. Specifically, all cluster assignments become similar when a degenerate solution is approached, bringing both the numerator and the denominator in (5) close to zero and creating numerical instability in the gradients. Adding small constants to avoid zero division can mitigate the issue only partially as it hinders the effect of the balancing term, which is what actually prevents degenerate solutions. Finally, we desire a loss that could be easily combined with other losses (e.g., the cross-entropy) when the cluster assignments are used to implement a graph pooling mechanism in a GNN architecture for graph classification (see Sec. 3.3). If the loss is combined, it is desirable to control the range of possible values it can assume and, therefore, a denominator taking arbitrary small values should be avoided.

To satisfy these requirements while retaining the desired properties of the objective function, we form a loss by adding the GTV and balancing terms rather than taking their ratio. First, we define the GTV loss term as

$$\mathcal{L}_{\text{GTV}}^* = \|\mathbf{S}\|_{\text{GTV}} = \sum_{k=1}^K \sum_{i=1}^N \sum_{j=i}^N a_{i,j} |s_{i,k} - s_{j,k}|, \quad (13)$$

Then, we define the asymmetrical norm term as

$$\mathcal{L}_{\text{AN}}^* = \sum_{k=1}^K \|\mathbf{s}_{:,k} - \text{quant}_{\rho}(\mathbf{s}_{:,k})\|_{1,\rho}. \quad (14)$$

To control the range of values of the loss, the two terms are rescaled as follows:

$$\mathcal{L}_{\text{GTV}} = \frac{\mathcal{L}_{\text{GTV}}^*}{2E} \in [0, 1], \quad (15)$$

$$\mathcal{L}_{\text{AN}} = \frac{\beta - \mathcal{L}_{\text{AN}}^*}{\beta} \in [0, 1], \quad (16)$$

where E is the number of edges in the graph and

$$\beta = \begin{cases} N\rho & \text{when } \rho = K - 1, \\ N\rho \min(1, K/(\rho + 1)) & \text{otherwise.} \end{cases} \quad (17)$$

The final loss reads:

$$\mathcal{L} = \alpha_1 \mathcal{L}_{\text{GTV}} + \alpha_2 \mathcal{L}_{\text{AN}}, \quad (18)$$

where $\alpha_1, \alpha_2 \in \mathbb{R}$ are hyperparameters that weigh the relative and total (in case there are other losses) contribution of the loss components.

The cluster assignments are computed by an MLP fed with the vertex representations produced by a stack of L MP layers

$$\mathbf{S} = \text{Softmax}(\text{MLP}(\mathbf{X}^{(L)}; \Theta_{\text{MLP}})) \quad (19)$$

As discussed in Sec. 2.3, common MP layers minimize the LQV of vertex features and the MLP, which is a smooth function, will naturally preserve the Laplacian smoothing effect when computing \mathbf{S} . While this was suitable for a SC objective, the optimization problem expressed by \mathcal{L}_{GTV} entails minimizing the ℓ_1 norm $\|\mathbf{s}_i - \mathbf{s}_j\|_1$ of each pair of adjacent vertices i and j . Thus, the MP layers should ideally minimize the discrepancy in the features of adjacent vertices in a ℓ_1 norm sense. To satisfy this requirement, we design a new MP layer starting from the definition of the GTV gradient.

3.2 The GTVConv layer

The GTV can be conveniently expressed by means of an incidence matrix (Wang et al., 2016) or a (nonlinear) ℓ_1 -Laplacian operator (Bai et al., 2018; Zhou and Schölkopf, 2005). In particular, let us define the GTV Laplacian as

$$\mathbf{L}_{\Gamma} = \mathbf{D}_{\Gamma} - \Gamma, \quad \text{with } \mathbf{D}_{\Gamma} = \text{diag}(\mathbf{\Gamma}\mathbf{1}) \quad (20)$$

where $\mathbf{\Gamma}$ is a connectivity matrix matching the sparsity pattern of the adjacency matrix, with elements

$$[\mathbf{\Gamma}]_{i,j} = \gamma_{i,j} = \frac{a_{i,j}}{\max\{|x_i - x_j|, \epsilon\}}, \quad (21)$$

where ϵ is a small value to ensure numerical stability. To minimize the GTV, we need to compute the sub-differential of $\|\mathbf{x}\|_{\text{GTV}}$ with respect to vertex i for some $\mathbf{x} \in \mathbb{R}^N$, which is given by

$$(\partial\|\mathbf{x}\|_{\text{GTV}})_i = \sum_{j=1}^N \gamma_{i,j} \cdot (x_i - x_j). \quad (22)$$

The full GTV gradient is given by (derivation in the supplementary):

$$\nabla(\|\mathbf{x}\|_{\text{GTV}}) = \mathbf{D}_{\Gamma}\mathbf{x} - \mathbf{\Gamma}\mathbf{x} = (\mathbf{D}_{\Gamma} - \mathbf{\Gamma})\mathbf{x} = \mathbf{L}_{\Gamma}\mathbf{x}. \quad (23)$$

Finally, $\|\mathbf{x}\|_{\text{GTV}}$ can be minimized by taking the following gradient descent update

$$\mathbf{x}^{(t+1)} = (\mathbf{I} - \delta\mathbf{L}_{\Gamma}^{(t)})\mathbf{x}^{(t)} \quad (24)$$

where δ is the step size. Interestingly, the update in (24) closely resembles the update in (8) and it can be implemented by a GCN operating on the connectivity matrix $\mathbf{I} - \delta\mathbf{L}_{\Gamma}^{(t)}$. We notice that the superscript (t) in $\mathbf{L}_{\Gamma}^{(t)}$ indicates the dependency on the features $\mathbf{x}^{(t)}$ in the denominator of (21). Without loss of generality, we replace index t which indicates the t -th step in the gradient descent update with index l , which indicates

the l -th MP layer in the GNN. Indeed, stacking GCN layers operating on $\mathbf{I} - \delta \mathbf{L}_\Gamma^{(l)}$ allows to gradually minimize $\|\mathbf{x}\|_{\text{GTV}}$.

The aggregation procedure in (24) is only valid for univariate vertex features $\mathbf{x} \in \mathbb{R}^N$. For a graph with multi-dimensional features $\mathbf{X} \in \mathbb{R}^{N \times F}$ the sub-differential is

$$(\partial \|\mathbf{X}\|_{\text{GTV}})_{i,f} = \sum_{j=1}^N \gamma_{i,j}^f \cdot (x_i^f - x_j^f), \quad (25)$$

where

$$\gamma_{i,j}^f = \frac{a_{i,j}}{\max\{|x_i^f - x_j^f|, \epsilon\}}, \quad f = 1, \dots, F. \quad (26)$$

The dependence on f means that an independent $\mathbf{\Gamma}^f$ is required for each feature and that the update in (24) must be done feature-wise. Notably, each time an MP layer maps the vertex features in a new F' -dimensional space, F' different connectivity matrices are required. Clearly, this implies two major drawbacks. First, building, storing, and applying many $\mathbf{\Gamma}^f$ matrices is computationally expensive, especially for large graphs. Second, since each feature is updated separately the trajectory followed by the optimizer during the gradient descent tends to be erratic and a longer time is required to reach convergence.

To address these issues, we simplify the gradient descent step by defining a single operator that computes the ℓ_1 distance of the whole feature vectors:

$$\hat{\gamma}_{i,j} = \frac{a_{i,j}}{\max\{\|\mathbf{x}_i - \mathbf{x}_j\|_1, \epsilon\}}. \quad (27)$$

By letting

$$\hat{\mathbf{L}}_\Gamma = \hat{\mathbf{D}}_\Gamma - \hat{\mathbf{\Gamma}}, \quad \text{with } [\hat{\mathbf{\Gamma}}]_{i,j} = \hat{\gamma}_{i,j} \quad \text{and } \hat{\mathbf{D}}_\Gamma = \text{diag}(\hat{\mathbf{\Gamma}}\mathbf{1}), \quad (28)$$

the vertex features update at step/layer $l + 1$ becomes

$$\mathbf{X}^{(l+1)} = \left(\mathbf{I} - \delta \hat{\mathbf{L}}_\Gamma^{(l)}\right) \mathbf{X}^{(l)}. \quad (29)$$

By referring to the notation of (7), the proposed GTVConv layer reads

$$\mathbf{X}^{(l+1)} = \sigma \left[\left(\mathbf{I} - \delta \hat{\mathbf{L}}_\Gamma\right) \mathbf{X}^{(l)} \Theta_{\text{MP}} \right] \quad (30)$$

Remarks There is a clear analogy between the LQV in (4), minimized by common MP layers, and the GTV defined in terms of \mathbf{L}_Γ , minimized by GTVConv. While the MP layers based on Laplacian smoothing perform low-pass filtering (Bo et al., 2021), GTVConv is closely related to graph trend filtering (Wang et al., 2016; Liu et al., 2021), which implements a total variation smoother based on the ℓ_1 Laplacian. While linear smoothers cannot handle heterogeneous smoothness, a total variation smoother encompasses both globally smooth functions, said to have homogeneous

smoothness, and functions with different levels of smoothness at different graph locations (Sadhanala et al., 2016). From the graph signal processing perspective, it means applying low- and high-pass filtering on the graph signal at the same time (Fu et al., 2022). In our case, when driven by the \mathcal{L}_{GTV} term in (18), GTVConv applies low-pass filtering to central vertices in the cluster and high-pass filtering at the clusters' edge, enabling sharp cluster transitions.

Similarly to attention-based GNNs (Veličković et al., 2017), GTVConv can learn edge weights in a data-driven fashion: by looking at (27), we notice that $\hat{\gamma}_{i,j}$ depend on the features $\mathbf{x}_i, \mathbf{x}_j$. Therefore, the output features at layer l will influence the edge weights at layer $l + 1$.

A variant to the proposed GTVConv layer is obtained from a GTV weighted by the vertex degrees, which gives an expression analogue to the LQV defined in terms of the symmetric normalized Laplacian (details in the supplementary).

3.3 TVGNN architectures for clustering and classification

In the following, we describe the GNN architectures we used in two downstream tasks: unsupervised vertex clustering and supervised graph classification.

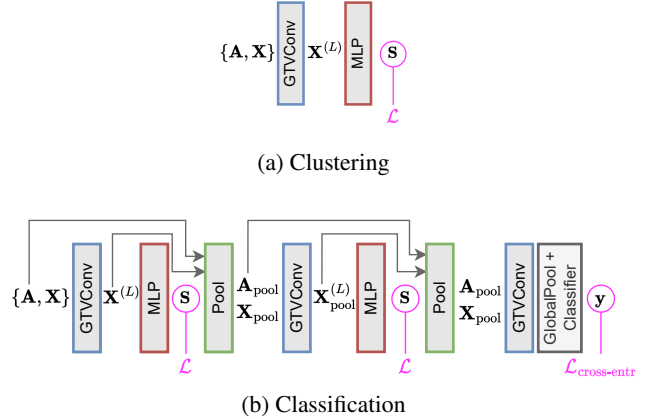


Figure 2: Schematic depiction of the architectures used for vertex clustering and graph classification.

Vertex clustering The GNN used for clustering is depicted in Fig. 2a. The architecture is rather simple: a stack of L GTVConv layers ($L \geq 1$) generates the feature vectors $\mathbf{X}^{(L)}$ that are used by an MLP to compute the cluster assignments \mathbf{S} . Since clustering is an unsupervised task, the GNN is trained using only the loss function \mathcal{L} defined in (18).

Graph classification Graph classification is a graph-level task, where a class label y_i is assigned to the i -th graph $\{\mathbf{A}_i, \mathbf{X}_i\}$. The GNN architectures for graph classification often alternate MP layers with graph pooling layers, which gradually distill the global label information from the vertex representations (Du et al., 2021).

The key and most challenging task in graph pooling is to generate a coarsened graph that summarizes well the properties of the original one (Grattarola et al., 2022). Similarly to previous work (Ying et al., 2018; Bianchi et al., 2020), the cluster assignment matrix \mathbf{S} computed in (19) is used to coarsen the adjacency matrix and compute pooled vertex features as

$$\mathbf{A}^{\text{pool}} = \mathbf{S}^T \tilde{\mathbf{A}} \mathbf{S} \in \mathbb{R}^{K \times K}; \mathbf{X}^{\text{pool}} = \mathbf{S}^T \mathbf{X} \in \mathbb{R}^{K \times F}. \quad (31)$$

According to a recently proposed taxonomy by Grattarola et al. (2022), our is a trainable, dense, fixed, hierarchical pooling method.

Graph pooling can be applied multiple times, to obtain smaller and smaller coarsened graphs. The features on the final coarsened graph are globally pooled and passed to a classifier that predicts the class label. A different instance of the loss in (18) is used to optimize the cluster assignments at each pooling layer. The total loss is given by combining the clustering losses, which in this case act as regularizers, and a supervised cross-entropy loss $\mathcal{L}_{\text{cross-entr}}$ between true and predicted class labels. Fig. 2b shows a schematic depiction.

By construction, the entry $a_{i,j}^{\text{pool}}$ of the coarsened adjacency \mathbf{A}^{pool} is the volume of edges between the elements assigned to clusters i and j . The minimization of \mathcal{L}_{GTV} pushes connected components to the same cluster, meaning that \mathbf{A}^{pool} gradually turns into a diagonally dominant matrix. Potentially, this poses issues if used as a connectivity matrix for aggregation in an MP layer, since the vertices will share information mostly with themselves, limiting the contribution of any MP layer operating on \mathbf{A}^{pool} . However, in the Laplacian (28) used by the GTVConv layer, the diagonal of the coarsened adjacency is removed, which avoids this potential problem.

4 Experiments

We evaluate the proposed TVGNN model on unsupervised vertex clustering and supervised graph classification tasks. The code to implement TVGNN is publicly available¹.

4.1 Unsupervised vertex clustering

In this experiment, we evaluate the capability of TVGNN to create cluster assignments that are sharp and match well the true vertex class.

The performance of TVGNN is compared against three classes of methods. The first, are algorithms that generate vertex embeddings based only on the adjacency matrix. The vertex embeddings are then clustered with k -means. Representatives of this category are Spectral Clustering (SC),

DeepWalk (Perozzi et al., 2014), Node2vec (Grover and Leskovec, 2016), and NetMF (Qiu et al., 2018). The second class of methods generates vertex embeddings by accounting both for the adjacency matrix and for the vertex features. Afterward, the learned embeddings are clustered with k -means. The chosen representatives for this category are the Graph AutoEncoder (GAE) and Variational Graph AutoEncoder (VGAE) (Kipf and Welling, 2016), and TADW (Yang et al., 2015). Finally, the last class of methods consists of end-to-end GNN models that directly generate soft cluster assignments \mathbf{S} by accounting both for the graph connectivity and the vertex features. In this case, k -means is not required and the discrete cluster assignments are simply obtained as $\mathbf{c} = \text{argmax}(\mathbf{S})$. DiffPool (Ying et al., 2018), DMoN (Tsitsulin et al., 2020), MinCutPool (Bianchi et al., 2020), and the proposed TVGNN belong to this class. The GNNs equipped with DiffPool, DMoN, and MinCutPool layers have the same general architecture of TVGNN depicted in Fig 2a, which is a stack of MP layers as in (7) followed by a layer that computes \mathbf{S} . The GNNs are trained only by minimizing unsupervised losses, such as those in Eq. 11 (MinCutPool), Eq. 12 (DMoN), and Eq. 18 (TVGNN). The hyperparameter configuration of each model is described in the supplementary material.

The methods are tested against three citation and one collaboration network (details in the supplementary). The number of clusters K is set to be equal to the number of vertex classes. Averaged results from 10 independent runs of each method are in Tab. 1, which reports the Normalized Mutual Information (NMI) and the accuracy (ACC) between the vertex labels and the cluster assignments sorted with the Kuhn-Munkres algorithm. Overall, TVGNN outperforms every other method in terms of both NMI and ACC.

The reported metrics give an indication of how well the clusters match the true vertex labels, but they do not measure the sharpness of the soft cluster assignment vectors generated by the GNN-based methods. To evaluate sharpness we compute the matrix $\mathbf{S}\mathbf{S}^T$. Let $\hat{\mathbf{y}}$ be the assignments obtained from the Kuhn-Munkres algorithm, which minimizes the mismatch between the discrete cluster assignments \mathbf{c} and the labels \mathbf{y} . By sorting the rows of \mathbf{S} according to the indices given by $\text{argsort}(\hat{\mathbf{y}})$, $\mathbf{S}\mathbf{S}^T$ will exhibit a block-diagonal structure if the vertices are assigned with high confidence to only one cluster, i.e., if the cluster assignments are sharp. In addition, the size of each block in $\mathbf{S}\mathbf{S}^T$ indicates the cluster size. Instead, if the assignments in \mathbf{S} are too smooth, non-zero elements will appear on the off-diagonal of $\mathbf{S}\mathbf{S}^T$. Fig. 3 shows $\log(\mathbf{S}\mathbf{S}^T)$ for the cluster assignments obtained for the Cora dataset (more results in the supplementary). The soft assignments given by TVGNN are much sharper than those computed by DiffPool, MinCutPool and DMoN, since most of the non-zero values lie within the blocks on the diagonal. Notably, the assignments given by DiffPool are so smooth that discerning any structure in $\mathbf{S}\mathbf{S}^T$ is impossible.

The cluster assignments are computed from vertex features

¹<https://github.com/FilippoMB/Total-variation-graph-neural-networks>

Table 1: NMI and ACC results for vertex clustering. Highest averages are in bold and second highest are underlined.

Method	Cora		Citeseer		Pubmed		DBLP		Tot. Average	
	NMI	ACC	NMI	ACC	NMI	ACC	NMI	ACC	NMI	ACC
SC	0.029±0.017	29.8±0.7	0.014±0.003	21.7±0.3	0.183±0.000	59.0±0.0	0.023±0.005	45.8±0.2	0.062	39.1
DeepWalk	0.064±0.024	23.0±2.1	0.005±0.001	19.4±0.3	0.001±0.000	36.1±0.1	0.001±0.000	26.7±0.1	0.018	26.3
node2vec	0.060±0.030	23.0±2.5	0.004±0.001	19.5±0.3	0.001±0.000	36.2±0.1	0.001±0.000	27.3±0.1	0.017	26.5
NetMF	0.251±0.000	38.9±0.0	0.127±0.000	27.7±0.0	0.059±0.000	44.8±0.0	0.037±0.000	45.6±0.0	0.119	39.3
TADW	0.012±0.000	19.3±0.0	0.002±0.000	18.8±0.0	0.031±0.000	42.8±0.0	0.012±0.000	29.8±0.0	0.014	27.7
GAE	0.328±0.051	46.5±6.2	0.163±0.029	38.1±3.8	<u>0.235±0.044</u>	58.9±7.2	0.111±0.029	41.6±3.5	0.209	46.3
VGAE	<u>0.437±0.029</u>	<u>57.2±5.4</u>	0.156±0.034	36.0±3.9	0.245±0.043	61.1±6.1	0.213±0.021	50.7±4.7	0.263	51.3
DiffPool	0.307±0.006	47.3±1.0	0.180±0.008	33.6±0.8	0.084±0.002	41.8±0.3	0.045±0.044	37.1±4.3	0.154	40.0
MinCutPool	0.406±0.029	53.4±4.1	<u>0.295±0.029</u>	<u>49.8±4.9</u>	0.209±0.015	57.3±3.5	0.297±0.025	53.8±3.4	<u>0.302</u>	<u>53.6</u>
DMoN	0.357±0.043	48.8±6.4	0.196±0.030	36.4±4.3	0.193±0.049	55.9±4.2	<u>0.335±0.027</u>	<u>59.0±4.0</u>	0.270	50.0
TVGNN	0.488±0.016	63.2±1.8	0.361±0.018	58.6±3.0	0.216±0.027	<u>60.0±2.0</u>	0.342±0.011	60.8±1.5	0.352	60.7

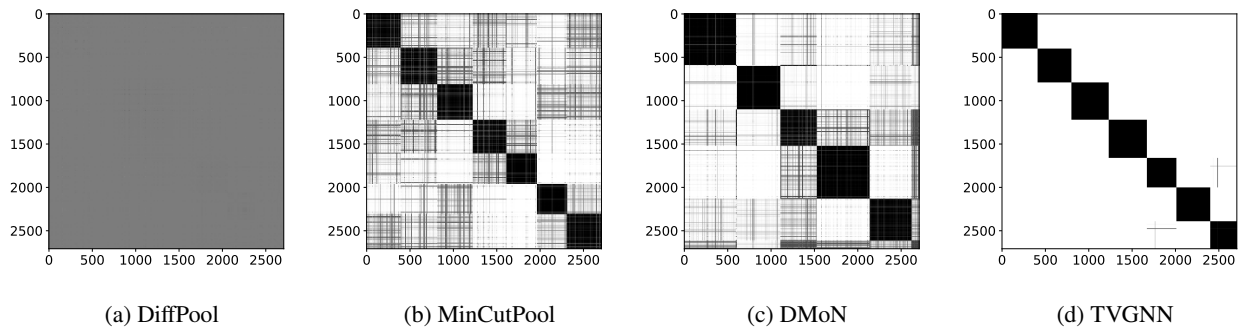
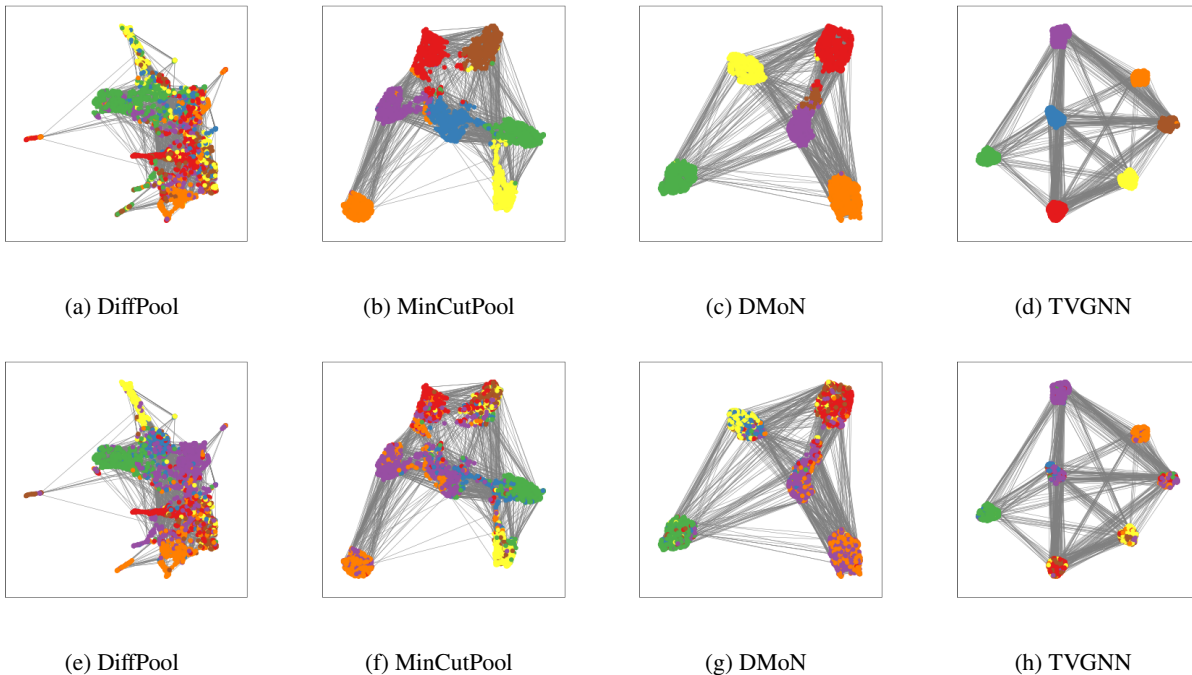
Figure 3: Visualization of the logarithm of SS^T for Cora.Figure 4: 2D UMAP transform of $\mathbf{X}^{(L)}$ for Cora with the edges from the original adjacency matrix. In (a)-(d) vertex colors correspond to cluster assignments \hat{y} from Kuhn-Munkres and in (e)-(h) colors correspond to the true labels.

Table 2: Graph classification accuracy. The highest mean accuracy for each dataset is in bold, and the second highest is underlined. We report the p -value of the difference between the two highest means (* and ** denote significance at 95% and 99% confidence levels).

Dataset	Top- K	SAGPool	DiffPool	MinCutPool	DMoN	TVGNN	p -value
Bench-easy	53.8 \pm 31.8	53.8 \pm 31.8	99.0 \pm 0.3	99.0 \pm 0.3	98.8 \pm 0.5	99.6 \pm 0.6	.011*
Bench-hard	30.5 \pm 0.7	29.5 \pm 0.0	<u>72.8</u> \pm 0.2	70.9 \pm 1.7	71.8 \pm 1.9	75.3 \pm 0.8	<.001**
MUTAG	77.5 \pm 8.4	76.8 \pm 9.7	<u>86.4</u> \pm 7.6	85.2 \pm 7.2	<u>86.7</u> \pm 7.0	88.4 \pm 7.5	.606
Mutagenicity	68.4 \pm 8.4	68.2 \pm 7.8	<u>78.5</u> \pm 1.5	78.4 \pm 1.4	<u>77.1</u> \pm 1.3	80.0 \pm 1.3	.028*
NCII	54.0 \pm 4.1	59.2 \pm 7.7	<u>74.1</u> \pm 1.8	<u>75.2</u> \pm 1.8	74.3 \pm 1.3	77.3 \pm 1.8	.018*
Proteins	69.6 \pm 2.7	70.4 \pm 2.5	74.6 \pm 4.2	<u>75.7</u> \pm 3.0	75.2 \pm 3.3	77.1 \pm 2.9	.302
D&D	62.0 \pm 5.6	64.2 \pm 7.0	77.7 \pm 3.0	<u>78.2</u> \pm 3.4	78.0 \pm 3.3	79.5 \pm 2.2	.323
COLLAB	73.4 \pm 6.9	75.6 \pm 2.5	78.4 \pm 1.6	<u>79.3</u> \pm 1.1	<u>79.5</u> \pm 0.7	79.8 \pm 1.1	.476
REDDIT-BINARY	54.0 \pm 10.0	50.0 \pm 0.1	80.9 \pm 2.7	82.3 \pm 3.2	<u>82.6</u> \pm 2.9	86.5 \pm 2.8	.007**

$\mathbf{X}^{(L)}$ generated by the last MP layer according to (19). To show the separation of the vertex communities before computing the assignments, we project $\mathbf{X}^{(L)}$ in two dimensions using UMAP (McInnes et al., 2018). Fig 4 shows the projected features for Cora (more results in the supplementary). In the first row, the vertices are colored according to the cluster assignments $\hat{\mathbf{y}}$ from Kuhn-Munkres; in the second row, according to the labels \mathbf{y} . Compared to the other methods, TVGNN yields clusters that are better separated and more compact. In addition, with TVGNN the class distribution is better aligned with the clustering partition.

4.2 Supervised graph classification

This task consists in assigning each graph \mathcal{G}_i to a class y_i . We adopt the deep architecture described in Sec. 3.3, where MP layers are interleaved with a pooling layer. To implement graph pooling, we consider DiffPool, MinCutPool, DMoN, SAGPool (Lee et al., 2019), Top- K (Cangea et al., 2018; Gao and Ji, 2019), and the proposed TVGNN. All GNN architectures follow the same general configuration depicted in Fig. 2b, with the main difference that TVGNN adopts GTVConv rather than standard MP layers (hyperparameters and other details in the supplementary). The unsupervised clustering losses in DiffPool, MinCutPool, DMoN, and TVGNN are computed at each pooling layer and then combined with the supervised cross-entropy loss at the end. The GNNs with SAGPool and Top- K do not have auxiliary losses and are trained only with the cross-entropy.

We consider 9 graph classification datasets (details in the supplementary). Training and testing is done with a stratified 5-fold train/test split. In addition, 10% of the training set is used as a validation set using a random stratified split. For each fold, we perform 3 independent runs and we train until we reach early stopping on the validation. To make the comparison fair, all methods are evaluated on the same data splits. The classification accuracy for each dataset is reported in Table 2. The GNN models based on TVGNN achieve the highest mean accuracy on all datasets. However, on MUTAG, Proteins, D&D, and COLLAB the differences between TVGNN and the second-best performing method

are not statistically significant.

5 Conclusions

We introduced a novel graph neural network approach that significantly improves the clustering performance of previous GNN models based on spectral clustering. We designed an unsupervised loss that minimizes the graph total variation of the cluster assignments to obtain compact and well-separated clusters. To facilitate the minimization of the loss, we introduced GTVConv, a message-passing layer that updates the vertex features by following the gradient of their graph total variation. The formal derivation demands GTVConv to use a different connectivity matrix to process each one of the vertex features, which is intractable. Therefore, we approximated the gradient descent step of GTV with a single connectivity matrix that accounts for all the vertex features at once. Despite the simplification, the proposed TVGNN model manages to separate very well the vertex features and generates sharp cluster assignments. In the experimental evaluation, TVGNN outperforms every other competing method in vertex clustering and graph classification tasks.

An appealing property of the GTVConv layer is the capability of adjusting the connectivity weights based on the vertex representations, which are learned in a data-driven fashion. In this work, the GTVConv was used in conjunction with the proposed unsupervised loss in GNN architectures for vertex clustering and graph classification. However, GTVConv could also be used as a stand-alone MP layer in GNNs for tasks such as semi-supervised vertex classification.

Acknowledgements

The authors gratefully acknowledge the support of Nvidia Corporation with the donation of the RTX A6000 GPUs used in this work.

References

- Bai, Y., Cheung, G., Liu, X., and Gao, W. (2018). Graph-based blind image deblurring from a single photograph. *IEEE Transactions on Image Processing*, 28(3):1404–1418.
- Bianchi, F. M. (2022). Simplifying clustering with graph neural networks. *arXiv preprint arXiv:2207.08779*.
- Bianchi, F. M., Gallicchio, C., and Micheli, A. (2022). Pyramidal reservoir graph neural network. *Neurocomputing*, 470:389–404.
- Bianchi, F. M., Grattarola, D., and Alippi, C. (2020). Spectral clustering with graph neural networks for graph pooling. In *International Conference on Machine Learning*, pages 874–883. PMLR.
- Bianchi, F. M., Grattarola, D., Livi, L., and Alippi, C. (2021). Graph neural networks with convolutional arma filters. *IEEE Transactions on Pattern Analysis and Machine Intelligence*.
- Bo, D., Wang, X., Shi, C., and Shen, H. (2021). Beyond low-frequency information in graph convolutional networks. In *Proceedings of the AAAI Conference on Artificial Intelligence*, volume 35, pages 3950–3957.
- Bresson, X., Laurent, T., Uminsky, D., and von Brecht, J. (2013). Multiclass total variation clustering. In Burges, C., Bottou, L., Welling, M., Ghahramani, Z., and Weinberger, K., editors, *Advances in Neural Information Processing Systems*, volume 26. Curran Associates, Inc.
- Cangea, C., Veličković, P., Jovanović, N., Kipf, T., and Liò, P. (2018). Towards sparse hierarchical graph classifiers. *arXiv preprint arXiv:1811.01287*.
- Du, J., Wang, S., Miao, H., and Zhang, J. (2021). Multi-channel pooling graph neural networks. In *IJCAI*, pages 1442–1448.
- Duval, A. and Malliaros, F. (2022). Higher-order clustering and pooling for graph neural networks. *arXiv preprint arXiv:2209.03473*.
- Fey, M. and Lenssen, J. E. (2019). Fast graph representation learning with pytorch geometric. *arXiv preprint arXiv:1903.02428*.
- Fu, G., Zhao, P., and Bian, Y. (2022). p -laplacian based graph neural networks. In *International Conference on Machine Learning*, pages 6878–6917. PMLR.
- Fu, X., Zhang, J., Meng, Z., and King, I. (2020). Magnn: Metapath aggregated graph neural network for heterogeneous graph embedding. In *Proceedings of The Web Conference 2020*, pages 2331–2341.
- Gao, H. and Ji, S. (2019). Graph u-nets. In *international conference on machine learning*, pages 2083–2092. PMLR.
- Grattarola, D. and Alippi, C. (2020). Graph neural networks in tensorflow and keras with spektral. *arXiv preprint arXiv:2006.12138*.
- Grattarola, D., Zambon, D., Bianchi, F. M., and Alippi, C. (2022). Understanding pooling in graph neural networks. *IEEE Transactions on Neural Networks and Learning Systems*.
- Grover, A. and Leskovec, J. (2016). node2vec: Scalable feature learning for networks. In *Proceedings of the 22nd ACM SIGKDD international conference on Knowledge discovery and data mining*.
- Hamilton, W. L. (2020). Graph representation learning. *Synthesis Lectures on Artificial Intelligence and Machine Learning*, 14(3):1–159.
- Hein, M. and Setzer, S. (2011). Beyond spectral clustering-tight relaxations of balanced graph cuts. In *NIPS*, pages 2366–2374. Citeseer.
- Ivanov, S., Sviridov, S., and Burnaev, E. (2019). Understanding isomorphism bias in graph data sets. *arXiv preprint arXiv:1910.12091*.
- Kampffmeyer, M., Løkse, S., Bianchi, F. M., Livi, L., Salberg, A.-B., and Jenssen, R. (2019). Deep divergence-based approach to clustering. *Neural Networks*, 113:91–101.
- Kipf, T. N. and Welling, M. (2016). Variational graph auto-encoders. *arXiv preprint arXiv:1611.07308*.
- Kipf, T. N. and Welling, M. (2017). Semi-supervised classification with graph convolutional networks. *International Conference of Learning Representations (ICLR)*.
- Klicpera, J., Bojchevski, A., and Günnemann, S. (2018). Predict then propagate: Graph neural networks meet personalized pagerank. *arXiv preprint arXiv:1810.05997*.
- Lee, J., Lee, I., and Kang, J. (2019). Self-attention graph pooling. In *International conference on machine learning*, pages 3734–3743. PMLR.
- Li, Q., Han, Z., and Wu, X.-M. (2018). Deeper insights into graph convolutional networks for semi-supervised learning. In *Thirty-Second AAAI conference on artificial intelligence*.
- Liu, X., Jin, W., Ma, Y., Li, Y., Liu, H., Wang, Y., Yan, M., and Tang, J. (2021). Elastic graph neural networks. In Meila, M. and Zhang, T., editors, *Proceedings of the 38th International Conference on Machine Learning*, volume 139 of *Proceedings of Machine Learning Research*, pages 6837–6849. PMLR.
- Ma, Y., Liu, X., Zhao, T., Liu, Y., Tang, J., and Shah, N. (2021). A unified view on graph neural networks as graph signal denoising. In *Proceedings of the 30th ACM International Conference on Information & Knowledge Management*, pages 1202–1211.
- McInnes, L., Healy, J., and Melville, J. (2018). Umap: Uniform manifold approximation and projection for dimension reduction. *arXiv preprint arXiv:1802.03426*.

- Min, E., Guo, X., Liu, Q., Zhang, G., Cui, J., and Long, J. (2018). A survey of clustering with deep learning: From the perspective of network architecture. *IEEE Access*, 6:39501–39514.
- Morris, C., Kriege, N. M., Bause, F., Kersting, K., Mutzel, P., and Neumann, M. (2020). TUDataset: A collection of benchmark datasets for learning with graphs. In *ICML 2020 Workshop on Graph Representation Learning and Beyond (GRL+ 2020)*.
- Nt, H. and Maehara, T. (2019). Revisiting graph neural networks: All we have is low-pass filters. *arXiv preprint arXiv:1905.09550*.
- Perozzi, B., Al-Rfou, R., and Skiena, S. (2014). Deepwalk: Online learning of social representations. In *Proceedings of the 20th ACM SIGKDD international conference on Knowledge discovery and data mining*.
- Qiu, J., Dong, Y., Ma, H., Li, J., Wang, K., and Tang, J. (2018). Network embedding as matrix factorization: Unifying deepwalk, line, pte, and node2vec. In *Proceedings of the 11th ACM international conference on web search and data mining*.
- Rangapuram, S. S., Mudrakarta, P. K., and Hein, M. (2014). Tight continuous relaxation of the balanced k-cut problem. In *NIPS*, pages 3131–3139.
- Rozemberczki, B., Kiss, O., and Sarkar, R. (2020). Karate Club: An API Oriented Open-source Python Framework for Unsupervised Learning on Graphs. In *Proceedings of the 29th ACM International Conference on Information and Knowledge Management (CIKM '20)*, page 3125–3132. ACM.
- Sadhanala, V., Wang, Y.-X., and Tibshirani, R. J. (2016). Total variation classes beyond 1d: Minimax rates, and the limitations of linear smoothers. *Advances in Neural Information Processing Systems*, 29.
- Shaham, U., Stanton, K., Li, H., Basri, R., Nadler, B., and Kluger, Y. (2018). Spectralnet: Spectral clustering using deep neural networks. In *International Conference on Learning Representations*.
- Su, X., Xue, S., Liu, F., Wu, J., Yang, J., Zhou, C., Hu, W., Paris, C., Nepal, S., Jin, D., et al. (2022). A comprehensive survey on community detection with deep learning. *IEEE Transactions on Neural Networks and Learning Systems*.
- Tian, F., Gao, B., Cui, Q., Chen, E., and Liu, T.-Y. (2014). Learning deep representations for graph clustering. In *Proceedings of the AAAI Conference on Artificial Intelligence*, volume 28.
- Tremblay, N., Gonçalves, P., and Borgnat, P. (2018). Design of graph filters and filterbanks. In *Cooperative and Graph Signal Processing*, pages 299–324. Elsevier.
- Tsitsulin, A., Palowitch, J., Perozzi, B., and Müller, E. (2020). Graph clustering with graph neural networks. *arXiv preprint arXiv:2006.16904*.
- Veličković, P., Cucurull, G., Casanova, A., Romero, A., Lio, P., and Bengio, Y. (2017). Graph attention networks. *arXiv preprint arXiv:1710.10903*.
- Von Luxburg, U. (2007). A tutorial on spectral clustering. *Statistics and computing*, 17(4):395–416.
- Wang, Y.-X., Sharpnack, J., Smola, A. J., and Tibshirani, R. J. (2016). Trend filtering on graphs. *Journal of Machine Learning Research*, 17(105):1–41.
- Wu, F., Souza, A., Zhang, T., Fifty, C., Yu, T., and Weinberger, K. (2019). Simplifying graph convolutional networks. In *International conference on machine learning*, pages 6861–6871. PMLR.
- Yang, C., Liu, Z., Zhao, D., Sun, M., and Chang, E. Y. (2015). Network representation learning with rich text information. *IJCAI'15*, page 2111–2117. AAAI Press.
- Yang, Z., Cohen, W. W., and Salakhutdinov, R. (2016). Revisiting semi-supervised learning with graph embeddings. *ICML'16*, page 40–48. JMLR.org.
- Ying, Z., You, J., Morris, C., Ren, X., Hamilton, W., and Leskovec, J. (2018). Hierarchical graph representation learning with differentiable pooling. *Advances in neural information processing systems*, 31.
- Zhou, D. and Schölkopf, B. (2005). Regularization on discrete spaces. In *Joint Pattern Recognition Symposium*, pages 361–368. Springer.

Supplementary material

A Detailed proofs and derivations

A.1 Graph cut in matrix form

To see that the cut between C_k and its conjugate \bar{C}_k can be expressed in matrix form, we first write the cut as

$$\text{cut}(C_k, \bar{C}_k) = \sum_{i \in C_k, j \in \bar{C}_k} a_{ij}(1 - z_i z_j),$$

where $z_i, z_j \in \{-1, 1\}$ are cluster indicators, i.e., $z_i = 1$ if vertex $i \in C_k$ and $z_i = -1$ if $i \notin C_k$.

Then,

$$\begin{aligned} \sum_{i,j} a_{ij}(1 - z_i z_j) &= \sum_{i,j} a_{ij} \left(\frac{z_i^2 + z_j^2}{2} - z_i z_j \right) \\ &= \frac{1}{2} \sum_i \left[\sum_j a_{ij} \right] z_i^2 + \frac{1}{2} \sum_j \left[\sum_i a_{ij} \right] z_j^2 - \sum_{i,j} a_{ij} z_i z_j \\ &= \frac{1}{2} \sum_i d_{ii} z_i^2 + \frac{1}{2} \sum_j d_{jj} z_j^2 - \mathbf{z}^T \mathbf{A} \mathbf{z} \\ &= \mathbf{z}^T \mathbf{D} \mathbf{z} - \mathbf{z}^T \mathbf{A} \mathbf{z} = \mathbf{z}^T \mathbf{L} \mathbf{z}. \end{aligned}$$

A.2 Derivation of the GTVConv aggregation

The i -th component of the sub-differential of $\|\mathbf{x}\|_{GTV}$ can be rewritten as

$$\begin{aligned} (\partial \|\mathbf{x}\|_{GTV})_i &= \sum_{j=1}^N \gamma_{i,j} (x_i - x_j) \\ &= x_i \sum_{j=1}^N \gamma_{i,j} - \sum_{j=1}^N \gamma_{i,j} x_j \\ &= x_i d_i - \sum_{j=1}^N \gamma_{i,j} x_j, \quad \text{where } d_i = \sum_j \gamma_{i,j} \\ &= \mathbf{D}_{\Gamma_i} \mathbf{x} - \mathbf{\Gamma}_i \mathbf{x}, \end{aligned}$$

where $\mathbf{\Gamma}_i$ and \mathbf{D}_{Γ_i} represent the i -th row of $\mathbf{\Gamma}$ and $\mathbf{D}_{\Gamma} = \text{diag}(\mathbf{\Gamma} \mathbf{1})$, respectively. The gradient of GTV of \mathbf{x} is then

$$\nabla(\|\mathbf{x}\|_{GTV}) = \mathbf{D}_{\Gamma} \mathbf{x} - \mathbf{\Gamma} \mathbf{x} = (\mathbf{D}_{\Gamma} - \mathbf{\Gamma}) \mathbf{x} = \mathbf{L}_{\Gamma} \mathbf{x},$$

Finally, the gradient descent step update for \mathbf{x} with step size δ is

$$\begin{aligned} \mathbf{x}^{(t+1)} &= \mathbf{x}^{(t)} - \delta \nabla(\|\mathbf{x}\|_{GTV})^{(t)} \\ &= \mathbf{x}^{(t)} - \delta \mathbf{L}_{\Gamma}^{(t)} \mathbf{x}^{(t)} \\ &= \left(\mathbf{I} - \delta \mathbf{L}_{\Gamma}^{(t)} \right) \mathbf{x}^{(t)}. \end{aligned}$$

A.3 Weighted LQV and GTV

Let us define the LQV weighted by the vertex degrees as

$$\|\mathbf{x}\|_{\text{LQV}_w} = \frac{1}{2} \sum_{i=1}^N \sum_{j=1}^N \left(\sqrt{\frac{a_{i,j}}{d_i}} x_i - \sqrt{\frac{a_{i,j}}{d_j}} x_j \right)^2 = \frac{1}{2} \sum_{i=1}^N \sum_{j=1}^N a_{i,j} \left(\frac{x_i}{\sqrt{d_i}} - \frac{x_j}{\sqrt{d_j}} \right)^2.$$

Then, we have that

$$\begin{aligned} (\partial \|\mathbf{x}\|_{\text{LQV}_w})_i &= \frac{1}{\sqrt{d_i}} \sum_j a_{i,j} \left(\frac{x_i}{\sqrt{d_i}} - \frac{x_j}{\sqrt{d_j}} \right) \\ &= \frac{x_i}{d_i} \sum_j a_{i,j} - \sum_j \frac{a_{i,j}}{\sqrt{d_i} \sqrt{d_j}} x_j \\ &= (\mathbf{I}\mathbf{x})_i - (\mathbf{D}^{-1/2} \mathbf{A} \mathbf{D}^{-1/2} \mathbf{x})_i \\ \nabla(\|\mathbf{x}\|_{\text{LQV}_w}) &= (\mathbf{I} - \mathbf{D}^{-1/2} \mathbf{A} \mathbf{D}^{-1/2}) \mathbf{x}, \end{aligned}$$

where $(\mathbf{I} - \mathbf{D}^{-1/2} \mathbf{A} \mathbf{D}^{-1/2})$ is the symmetrically normalized Laplacian.

If we compute the gradient descent update we obtain

$$\begin{aligned} \mathbf{x}^{(t+1)} &= \mathbf{x}^{(t)} - \delta \nabla(\|\mathbf{x}\|_{\text{LQV}_w})^{(t)} \\ &= \mathbf{x}^{(t)} - \delta (\mathbf{I} - \mathbf{D}^{-1/2} \mathbf{A} \mathbf{D}^{-1/2}) \mathbf{x}^{(t)}. \end{aligned}$$

When the gradient step size is $\delta = 1$, we get

$$\mathbf{x}^{(t+1)} = \mathbf{D}^{-1/2} \mathbf{A} \mathbf{D}^{-1/2} \mathbf{x}^{(t)},$$

which closely resembles the aggregation function used by a GCN to update the vertex features.

Now, let us define the degree-weighted GTV as

$$\|\mathbf{x}\|_{\text{GTV}_w} = \sum_{i=1}^N \sum_{j=1}^N \left| \sqrt{\frac{a_{i,j}}{d_i}} x_i - \sqrt{\frac{a_{i,j}}{d_j}} x_j \right| = \sum_{i=1}^N \sum_{j=1}^N |q_{i,j}|,$$

with $q_{i,j} = \sqrt{\frac{a_{i,j}}{d_i}} x_i - \sqrt{\frac{a_{i,j}}{d_j}} x_j$ and $d_i = \mathbf{D}_{ii}$, where $\mathbf{D} = \text{diag}(\mathbf{A}\mathbf{1})$. The numerically stable subdifferential is now given by

$$(\partial \|\mathbf{x}\|_{\text{GTV}_w})_{i,j}^\epsilon = \begin{cases} \sqrt{\frac{a_{i,j}}{d_i}} \cdot \frac{q_{i,j}}{|q_{i,j}|}, & |q_{i,j}| \geq \epsilon \\ \sqrt{\frac{a_{i,j}}{d_i}} \cdot \frac{q_{i,j}}{\epsilon}, & |q_{i,j}| < \epsilon \end{cases}$$

which can be rewritten in a more compact form as

$$(\partial \|\mathbf{x}\|_{\text{GTV}_w})_i^\epsilon = \sum_j \sqrt{\frac{a_{i,j}}{d_i}} \frac{q_{i,j}}{\max\{\epsilon, |q_{i,j}|\}} = \sum_j \frac{a_{i,j}}{\sqrt{d_i}} \frac{\frac{x_i}{\sqrt{d_i}} - \frac{x_j}{\sqrt{d_j}}}{\max\{\epsilon, |q_{i,j}|\}}.$$

Now let

$$\gamma_{i,j} = \frac{a_{i,j}}{\max\{\epsilon, |q_{i,j}|\}}$$

By substituting $\gamma_{i,j}$ we get

$$\begin{aligned}
 (\partial \|\mathbf{x}\|_{\text{GTV}_w})_i^\epsilon &= \sum_j \frac{1}{\sqrt{d_i}} \gamma_{i,j} \left(\frac{x_i}{\sqrt{d_i}} - \frac{x_j}{\sqrt{d_j}} \right) \\
 &= \frac{x_i}{d_i} \sum_j \gamma_{i,j} - \sum_j \frac{\gamma_{i,j}}{\sqrt{d_i} \sqrt{d_j}} x_j \\
 &= (\mathbf{D}^{-1} \mathbf{D}_\Gamma)_i \mathbf{x} - (\mathbf{D}^{-1/2} \mathbf{\Gamma} \mathbf{D}^{-1/2})_i \mathbf{x} \\
 &= (\mathbf{D}^{-1/2} \mathbf{D}_\Gamma \mathbf{D}^{-1/2})_i \mathbf{x} - (\mathbf{D}^{-1/2} \mathbf{\Gamma} \mathbf{D}^{-1/2})_i \mathbf{x},
 \end{aligned}$$

where $\mathbf{D}_\Gamma = \text{diag}(\mathbf{\Gamma} \mathbf{1})$.

The gradient of the weighted GTV is

$$\begin{aligned}
 \nabla(\|\mathbf{x}\|_{\text{GTV}_w}) &= \mathbf{D}^{-1/2} \mathbf{D}_\Gamma \mathbf{D}^{-1/2} \mathbf{x} - \mathbf{D}^{-1/2} \mathbf{\Gamma} \mathbf{D}^{-1/2} \mathbf{x} \\
 &= \mathbf{D}^{-1/2} (\mathbf{D}_\Gamma - \mathbf{\Gamma}) \mathbf{D}^{-1/2} \mathbf{x} \\
 &= \mathbf{D}^{-1/2} \mathbf{L}_\Gamma \mathbf{D}^{-1/2} \mathbf{x}
 \end{aligned}$$

A gradient descent step for minimizing the weighted GTV is given by

$$\begin{aligned}
 \mathbf{x}^{(t+1)} &= \mathbf{x}^{(t)} - \delta \nabla(\|\mathbf{x}\|_{\text{GTV}_w})^{(t)} \\
 &= \mathbf{x}^{(t)} - \delta \mathbf{D}^{-1/2} \mathbf{L}_\Gamma^{(t)} \mathbf{D}^{-1/2} \mathbf{x}^{(t)} \\
 &= (\mathbf{I} - \delta \mathbf{D}^{-1/2} \mathbf{L}_\Gamma^{(t)} \mathbf{D}^{-1/2}) \mathbf{x}^{(t)}
 \end{aligned}$$

which is equivalent to the aggregation step of a GCN with $\tilde{\mathbf{A}} = \mathbf{I} - \delta \mathbf{D}^{-1/2} \mathbf{L}_\Gamma^{(t)} \mathbf{D}^{-1/2}$.

We notice the analogy between the updates derived from the degree-weighted LQV $\mathbf{x}^{(t+1)} = \mathbf{x}^{(t)} - \delta (\mathbf{I} - \mathbf{D}^{-1/2} \mathbf{A} \mathbf{D}^{-1/2}) \mathbf{x}^{(t)}$ and from the degree-weighted GTV $\mathbf{x}^{(t+1)} = (\mathbf{I} - \delta \mathbf{D}^{-1/2} \mathbf{L}_\Gamma^{(t)} \mathbf{D}^{-1/2}) \mathbf{x}^{(t)}$.

B Details of the experimental setting

B.1 Software libraries

The GNN models were implemented using Spektral² (Grattarola and Alippi, 2020). The methods for vertex embedding used in the vertex clustering experiment are based on the Karateclub³ (Rozemberczki et al., 2020) implementation, and most of the datasets are taken from Pytorch Geometric⁴ (Fey and Lenssen, 2019).

B.2 Datasets details

In the vertex clustering experiment, we analyzed the citation networks Cora, Pubmed, Citeseer (Yang et al., 2016) and DBLP (Fu et al., 2020). In the graph classification experiment, we analyzed seven TUD datasets (Morris et al., 2020) and two synthetic datasets, Bench-easy and Bench-hard (Bianchi et al., 2022).

Details about the datasets are reported in Tab. 3 and 4. In the graph classification datasets, the vertex feature matrix \mathbf{X} consists of vertex attributes, vertex labels, or a concatenation of both. For the datasets where neither the vertex attributes nor the vertex labels are available, a one-hot encoded vertex degree matrix was used as a surrogate feature for \mathbf{X} . Furthermore, motivated by the work of Ivanov et al. (2019), the datasets were cleaned such that they only contained non-isomorphic graphs.

Table 3: Details of the vertex clustering datasets.

Dataset	#Vertices	#Edges	#Vertex attr.	#Vertex classes
Cora	2,708	10,556	1,433	7
Citeseer	3,327	9,104	3,703	6
Pubmed	19,717	88,648	500	3
DBLP	17,716	105,734	1,639	4

Table 4: Details of the graph classification datasets.

Dataset	#Samples	#Classes	Avg. #vertices	Avg. #edges	Vertex attr.	Vertex labels
Bench-easy	1,800	3	147.82	922.67	–	yes
Bench-hard	1,800	3	148.32	572.32	–	yes
MUTAG	188	2	17.93	19.79	–	yes
Mutagenicity	4,337	2	30.32	61.54	–	yes
NCII	4,110	2	29.87	64.60	–	yes
Proteins	1,113	2	39.06	72.82	1	yes
D&D	1,178	2	284.32	1,431.32	–	yes
COLLAB	5,000	3	74.49	4,914.43	–	no
REDDIT-BINARY	2,000	2	429.63	995.51	–	no

Table 5: Hyperparameters configuration for the vertex clustering and graph classification tasks. σ_{MP} indicates the activation of the MP layers, σ_{MLP} is the activation of the MLP layers, δ is the step-size in the GTVConv layer, α_1 is the coefficient for the total variation loss \mathcal{L}_{GTV} , α_2 is the coefficient for the balance loss \mathcal{L}_{AN} , ℓ_2 indicates the weight of the ℓ_2 regularization on the GNN weight parameters,

Parameters	Vertex Clustering	Bench-easy	Bench-hard	MUTAG	Mutagenicity
# MP layers	2	1	1	1	2
# MP channels	512	32	32	32	16
σ_{MP}	ELU	ReLU	ReLU	ELU	ReLU
δ	0.311	0.724	2.288	1.644	1.078
# MLP layers	1	3	1	3	2
# MLP channels	256	64	64	64	256
σ_{MLP}	ReLU	ReLU	ReLU	ReLU	ReLU
α_1	0.785	0.594	0.188	0.623	0.367
α_2	0.514	0.974	0.737	0.832	0.752
ℓ_2	–	1e-5	0	1e-4	1e-5
Learning rate	1e-3	1e-3	5e-4	1e-2	1e-3

Parameters	NCII	Proteins	D&D	COLLAB	REDDIT-BINARY
# MP layers	3	3	1	2	3
# MP channels	32	64	64	256	16
σ_{MP}	ReLU	ELU	ELU	ReLU	ReLU
δ	2.411	2.073	0.622	0.554	1.896
# MLP layers	3	1	2	2	3
# MLP channels	32	16	32	128	16
σ_{MLP}	ReLU	ELU	ReLU	ReLU	ReLU
α_1	0.936	0.985	0.354	0.304	0.654
α_2	0.639	0.751	0.323	0.801	0.962
ℓ_2	1e-3	1e-3	1e-5	0	1e-3
Learning rate	5e-4	1e-3	1e-5	5e-5	1e-3

B.3 Hyperparameters configuration

The hyperparameters for TVGNN for both the vertex clustering and graph classification tasks are reported in Tab. 5. The parameter ϵ which ensures numerical stability for Γ was set to $1e-3$ in all experiments. For MinCutPool (Bianchi et al., 2020), GAE and VGAE (Kipf and Welling, 2016) the model configurations are those reported in the original papers. For DiffPool, Top- K , and SAGPool configurations were the same as in (Bianchi et al., 2020). The models with DMoN used the same hyperparameter configuration as for MinCutPool and the regularization term \mathcal{L}_r in the auxiliary loss is weighted by $1e-1$. In the case of DeepWalk, node2vec, NetMF, and TADW we used the default configurations from the Karateclub library (Rozemberczki et al., 2020).

For the graph classification task, the GNNs with TVGNN, MinCutPool, DiffPool, and DMoN were trained with a batch size of 8 for all datasets, except D&D and REDDIT-BINARY, for which batch size was set to 1 due to memory constraints. The models with Top- K and SAGPool were trained with a batch size of 1 for all datasets. For the vertex clustering task, the GNNs were trained for 10,000 epochs. In the graph classification task, we performed early stopping on the validation set using a patience of 20 epochs.

C Additional results

C.1 Additional plots

Plots with the logarithm of $\mathbf{S}\mathbf{S}^T$ and the UMAP transform of $\mathbf{X}^{(L)}$ for Citeseer, Pubmed and DBLP are presented in Fig. 5 and 6, respectively. As for the case of Cora, TVGNN manages to give better separated clusters with sharper assignments for all three graphs when compared to the other three GNN-based clustering methods that produce soft assignments.

C.2 Clustering two simple point clouds

Fig. 7 and 8 show the largest soft assignment for each node when tasked with clustering a 2D ring graph and a 2D grid graph, respectively. The color of the node is chosen such that a sharp assignment of 1 gives a bright color (lightness equal to 0.5), while smoother assignments give paler colors, and an assignment of 0 is just white (lightness equal to 1). The number of desired clusters K for the ring and grid was 5 and 10, respectively. The models were trained using the same hyperparameters as for the vertex classification task in the experiments.

Again we see that DiffPool gives smooth assignments resulting in noticeably paler colors. In MinCutPool and DMoN we observe paler colors in the proximity of the cluster borders, while TVGNN exhibits sharp transitions from one cluster to the other. We also notice that TVGNN is the only method that on the grid generates a partition with the desired number of clusters $K = 10$.

To better quantify the sharpness of the transition between different clusters, in Fig. 9a we show the largest value in the soft assignment vectors for the ring when moving along it. Here, the differences in cluster transitions are clear: the drops in the assignment value indicate the presence of smooth transitions. The cluster assignments of Diffpool are always very smooth; MinCutPool and DMoN exhibit smooth assignments only when crossing from one cluster to the other; with TVGNN the assignments are always sharp.

A similar plot for the grid is presented in Fig. 9b, but here the largest soft assignments for all nodes are sorted from lowest to highest, which indicates the overall proportion of smooth assignments. Also in this case, the cluster assignments of TVGNN are the sharpest, followed by DMoN, MinCutPool, and Diffpool.

²<https://graphneural.network>

³<https://karateclub.readthedocs.io>

⁴<https://pytorch-geometric.readthedocs.io>

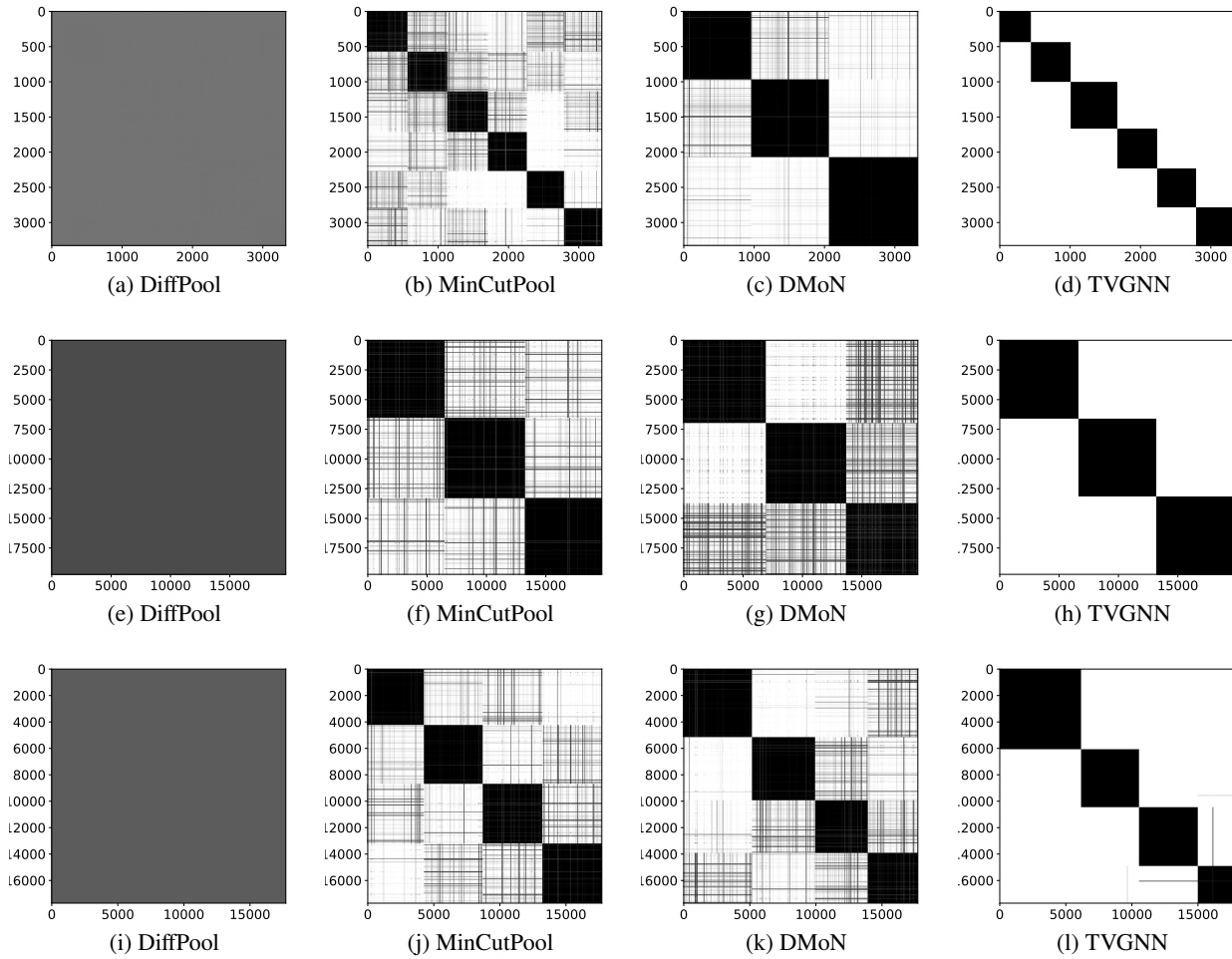


Figure 5: Logarithm of SS^T for Citeseer: (a)-(d), Pubmed: (e)-(h), and DBLP: (i)-(l).

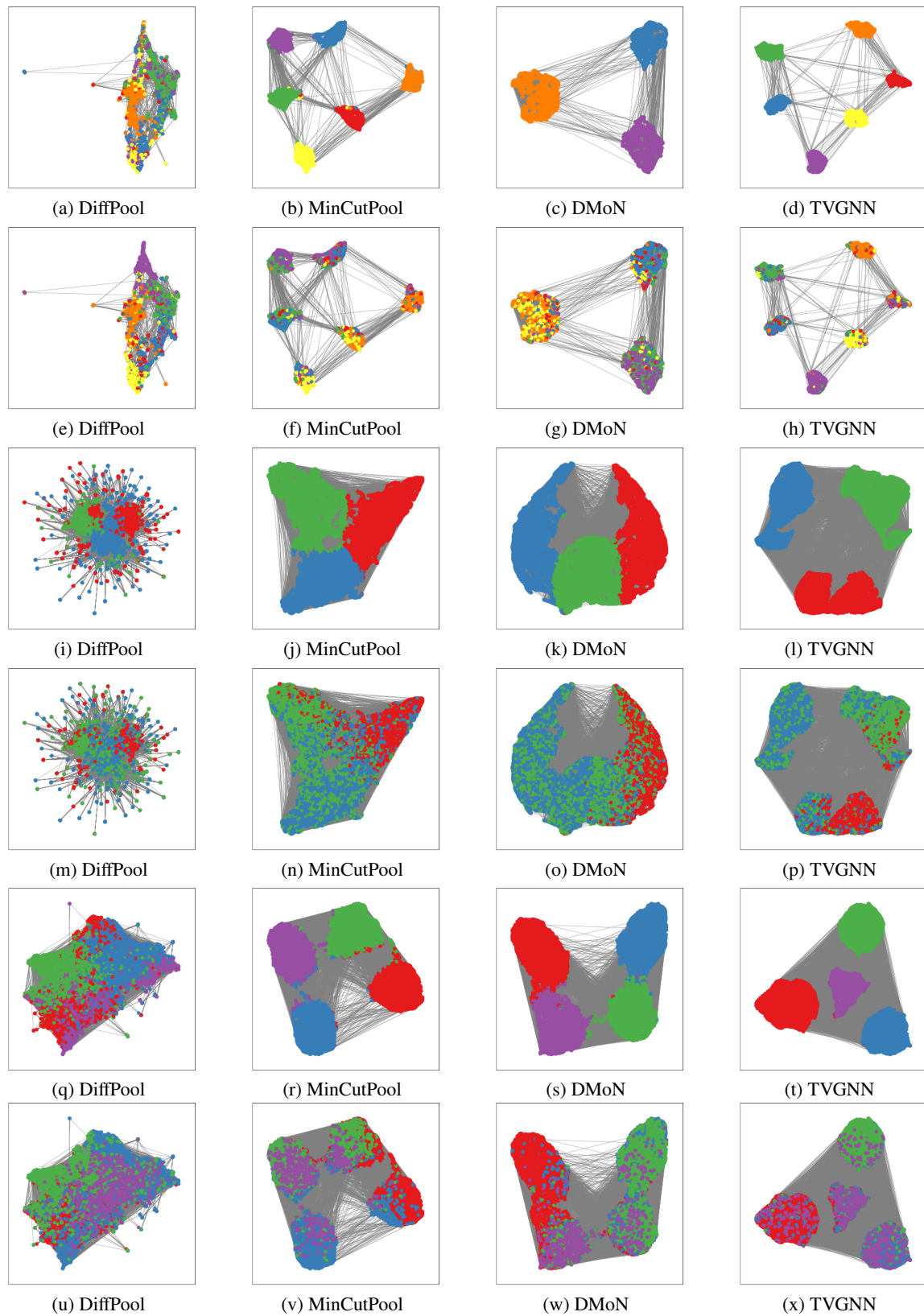


Figure 6: UMAP transforms of $\mathbf{X}^{(L)}$ for CiteSeer: (a)-(h), Pubmed: (i)-(p), and DBLP: (q)-(x). Colors in the top row of each dataset correspond to cluster assignments, while the colors in the bottom row correspond to true labels.

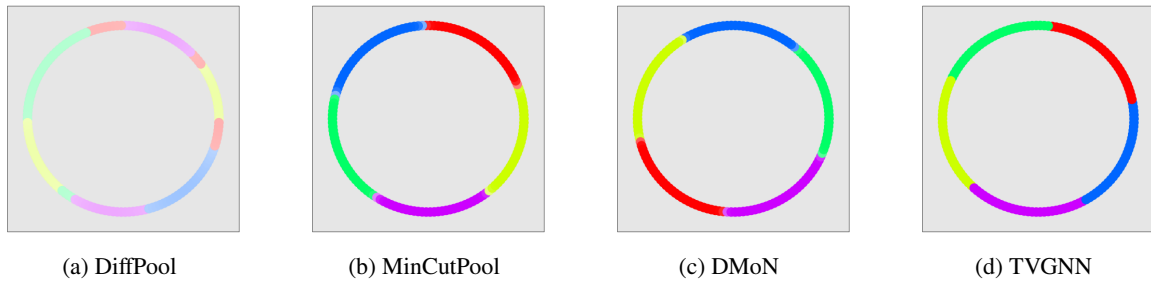


Figure 7: Cluster assignments for the ring graph. The colors correspond to the index of the largest value in the soft cluster assignment vector. The brightness is proportional to the highest value in the assignment vector.

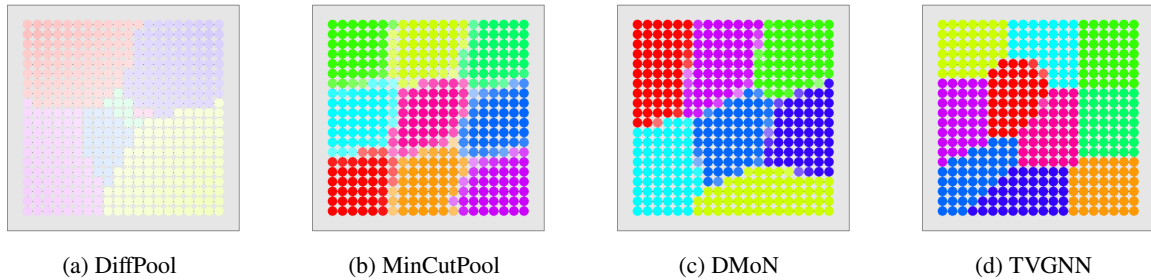


Figure 8: Cluster assignments for the grid graph. The colors correspond to the index of the largest value in the soft cluster assignment vector. The brightness is proportional to the highest value in the assignment vector.

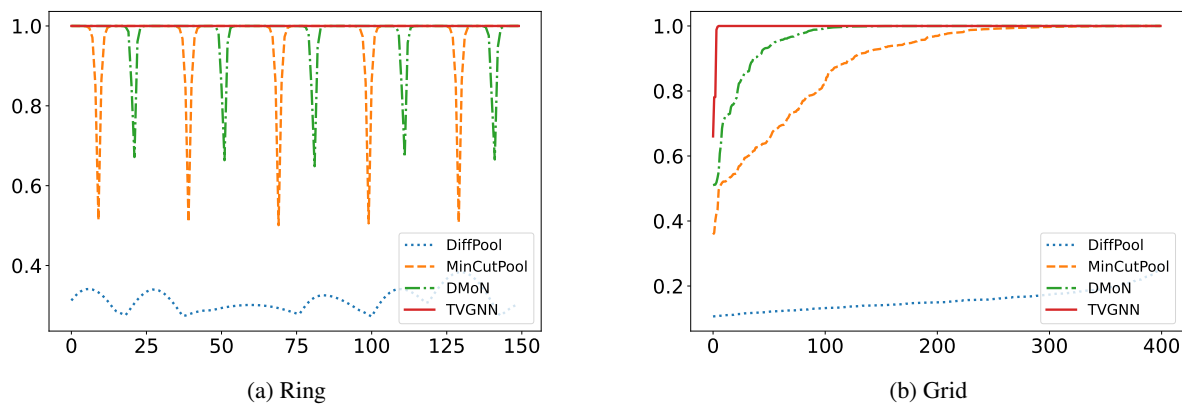


Figure 9: Largest value in the soft cluster assignment vector as a function of the vertex index. For the ring in (a), the horizontal axis moves along the circumference of the ring. For the grid in (b), the node indices are sorted according to the largest value in the assignment vectors.